Inorg. Chem. **2003**, *42*, 4299–4307

Templating Schiff-Base Lateral Macrobicycles: An Experimental and Theoretical Structural Study of the Intermediates

Carlos Platas-Iglesias, David Esteban, Vicente Ojea, Fernando Avecilla, Andrés de Blas,* and Teresa Rodríguez-Blas*

Departamento de Química Fundamental, Universidade da Coruña, Campus da Zapateira s/n 15071 A Coruña, Spain

Received March 11, 2003

In this paper, we report a structural study both in the solid state and in solution of barium complexes with the diamine *N*,*N*′-bis(2-aminobenzyl)-4,13-diaza-18-crown-6 (**L²**), that allows us to rationalize the template effect of the metal ion in the synthesis of Schiff-base lateral macrobicycles resulting from the condensation of **L²** with different dicarbonyl compounds. The X-ray crystal structures of [Ba(**L²**)(ClO_4)](ClO_4) (**3**) [triclinic space group $P\bar{1}$ with $Z = 2$, $a = 10.467(2)$ Å, $b = 10.4755(2)$ Å, $c = 16.9911(3)$ Å, $\alpha = 85.075(1)°$, $\beta = 80.907(1)°$, and $\gamma = 61.627(4)°$] and [Ba(**L²**)(NCS)(H_2O)](SCN) (**4**) [monoclinic space group $P2_1/n$ with $Z = 4$, $a = 9.954(5)$ Å, $b = 29.193(5)$ Å, $c = 11.313(5)$ Å, and $\beta = 91.371(5)°$] demonstrate that in the solid state the barium(II) ion induces an *anti* conformation of the receptor in the complexes. Variable temperature ^{1}H and ^{13}C NMR data point out that in solution compounds **3** and **4** exist as a mixture of *syn* and *anti* isomers. The presence of the *syn* isomer in solution, independent of the counterion employed (perchlorate or thiocyanate), accounts for the effectiveness of the barium(II) ion as a template agent in the synthesis of the lateral macrobicycles resulting from the condensation of **L²** with different dicarbonyl compounds. Density functional theory calculations (at the B3LYP/LanL2DZ level) for [Ba(**L²**)]$^{2+}$ predict the *syn* conformation to be more stable both in vacuo and in solution (PCM model). In order to asses which of the two isomers predominates in acetonitrile solution, the ^{13}C NMR shielding tensors of the two isomers of [Ba(**L²**)]$^{2+}$ were calculated for the in vacuo optimized structures by using the GIAO method, and the results were compared with the experimental ones. According to these analyses, a *syn* stereochemistry is assigned to the major species in solution.

Introduction

The direct synthesis of a free macrocycle from its organic precursors often results in a low yield of the desired cyclic product, with side reactions such as polymerization predominating. Consequently, some synthetic strategies such as the use of high dilution conditions, the incorporation of a rigid group in the open chain precursors, and the use of template agents have been developed. The routine use of metal template procedures for obtaining a wide range of macrocyclic systems stems from 1960 when Curtis discovered a template reaction for obtaining an isomeric pair of nickel macrocyclic complexes.[1] Nowadays, there are a large number of metal template syntheses of macrocyclic products, and such in situ procedures have proven to be of major synthetic significance over time. The metal template effect has been studied for some specific systems, and the possible roles for the metal ion in a template reaction have been established: First, the metal ion may sequester the cyclic product from an equilibrium mixture promoting the macrocycle as its metal complex (thermodynamic template effect). Second, the metal ion may direct the steric course of a condensation facilitating the formation of the required cyclic product (kinetic template effect).[2−4] This effect is especially pronounced when rigid building blocks are used, and relatively rigid macrocycles are formed. In such cases, conformational changes within the macrocyclic ligand are

* Corresponding authors. E-mail: mayter@udc.es (T.R.-B.); ucambv@udc.es (A.d.B.).

(1) Curtis, N. F. *J. Chem. Soc.* **1960**, 4409.

(2) Thompson, M. C.; Busch, D. H. *J. Am. Chem. Soc.* **1964**, *86*, 3651.

(3) Busch, D. H.; Cairns, C. In *Progress in Macrocyclic Chemistry*; Izatt, R. M., Christensen, J. J. Eds.; J. Wiley & Sons: New York, 1987; Vol. 3.

(4) Lindoy, L. F. *The Chemistry of Macrocyclic Ligand Complexes*; Cambridge University Press: Cambridge, 1989.

10.1021/ic034266t CCC: $25.00
Published on Web 06/13/2003

Chart 1

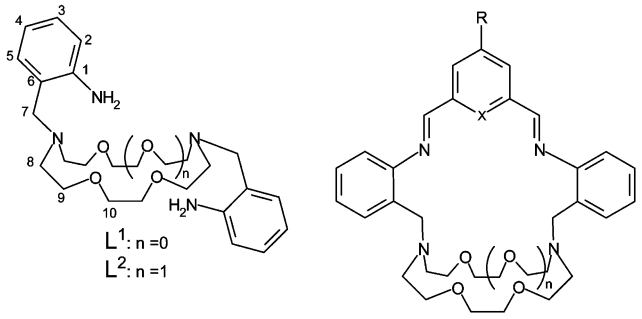

limited, and little adjustment of the coordination sphere geometry is possible.

Template Schiff-base condensations between dicarbonyl compounds and diamines are among the simplest and most popular methods for macrocycle synthesis.[5] A variety of metal ions were found to be effective templates for these systems, including alkaline,[6] alkaline earth,[7] first row transition,[8] Pb(II),[9,10] Ag(I),[11] Cd(II),[12] and lanthanide(III) metal ions.[13] In a previous work, we reported the synthesis of the lateral macrobicycles $\mathbf{L^3}-\mathbf{L^6}$ (shown in Chart 1), that are the first examples of Schiff-base lateral macrobicycles, and which derive from the condensation of the diamine precursor [*N*,*N*′-bis(2-aminobenzyl)-1,10-diaza-15-crown-5 ($\mathbf{L^1}$) or *N*,*N*′-bis(2-aminobenzyl)-4,13-diaza-18-crown-6 ($\mathbf{L^2}$)] and the corresponding dialdehyde (2,6-diformylpyridine or 2,6-diformyl-4-methylphenol).[14] We have found that they cannot be prepared by direct reaction between the organic precursors due to the *anti* arrangement adopted by the diamines ($\mathbf{L^1}$ or $\mathbf{L^2}$), but barium can act as an effective template, thereby facilitating the formation of the desired macrobicycles in high yields. In this case, the template effectiveness of barium(II) or any other metal ion comes from its ability to orient the pendant arms of $\mathbf{L^1}$ and/or $\mathbf{L^2}$ to a *syn* conformation. Experimental evidence for this conformation was found both in the solid state and in solution for the barium complexes with precursor $\mathbf{L^1}$ ($[Ba(\mathbf{L^1})](ClO_4)_2$ (compound **1**) and $[Ba(\mathbf{L^1})(NCS)_2]$ (compound **2**)), which are intermediates in the formation of macrobicycles $\mathbf{L^3}$ and $\mathbf{L^4}$.[14,15] In the present paper, we report an experimental and DFT (density functional theory) structural study on the barium complexes with $\mathbf{L^2}$ ($[Ba(\mathbf{L^2})(ClO_4)](ClO_4)$ (compound **3**) and $[Ba(\mathbf{L^2})(H_2O)(NCS)](SCN)$ (compound **4**)) in order to rationalize the template effect of this metal ion in the synthesis of macrobicycles $\mathbf{L^5}$ and $\mathbf{L^6}$. Theoretical investigation represents a valid tool to understand the structure, dynamics, stability, and NMR properties of alkaline and alkaline earth complexes.[16] In particular, DFT has been revealed to be a useful tool to model this type of compound both in vacuo and in solution.[17] The $[Ba(\mathbf{L^2})]^{2+}$ system is characterized by means of DFT methods (at the B3LYP/LanL2DZ level of theory), and the obtained results are compared with the solid state structures of compounds **3** and **4**. As the template reactions for the synthesis of the macrobicycles occur in solution, we have performed DFT calculations both in vacuo and in solution, the latter by using the polarizable continuum model (PCM), that offers a balanced and theoretically sound treatment of all solute−solvent interactions at a very reasonable computational cost, even at the DFT level. The ^{13}C NMR shielding tensors of the two isomers of $[Ba(\mathbf{L^2})]^{2+}$ were calculated on the in vacuo optimized structures by using the GIAO method, and the results were compared with the experimental ones.

Experimental Section

Materials. Compounds of formula $[Ba(\mathbf{L^1})](ClO_4)_2$ (**1**), $[Ba(\mathbf{L^1})(NCS)_2]$ (**2**), $[Ba(\mathbf{L^2})(ClO_4)](ClO_4)$ (**3**), $[Ba(\mathbf{L^2})(H_2O)(NCS)](SCN)$ (**4**), and $[Pb(\mathbf{L^2})](ClO_4)_2$ were prepared as previously described.[14,18] All other chemicals were purchased from commercial sources and used without further purification. Solvents were of reagent grade purified by the usual methods. X-ray quality crystals of **3** and **4** were grown by slow diffusion of diethyl ether into a solution of the corresponding compound in acetonitrile.

Caution! Although we have experienced no difficulties with the perchlorate salts, these should be regarded as potentially explosive and handled with care.[19]

Physical Measurements. ^1H and ^{13}C NMR spectra were run on a Bruker AC 200 F or a Bruker WM-500 spectrometer. Electronic spectra in the UV−vis range were recorded at 20 °C on a Perkin-Elmer Lambda 900 UV−vis spectrophotometer using 1.0 cm quartz

(5) (a) Nelson, S. M. *Pure Appl. Chem.* **1980**, *52*, 2461. (b) Fenton, D. E.; Vigato, P. A. *Chem. Soc. Rev.* **1988**, *17*. 69. (c) Collinson, S. R.; Fenton, D. E. *Coord. Chem. Rev.* **1996**, *148*, 19.
(6) Drew, M. G. B.; Howarth, O. W.; Harding, C. J.; Martin, N.; Nelson, J. *J. Chem. Soc., Chem. Commun*. **1995**, 903.
(7) (a) Bailey, N. A.; Rodríguez de Barbarín, C. O.; Fenton, D. E.; Hellier, P. C.; Hempstead, P. D.; Kanesato, M.; Leeson, P. B. *J. Chem. Soc., Dalton Trans*. **1995**, 765. (b) Drew, M. G. B.; Nelson, J.; Nelson, S. M. *J. Chem. Soc., Dalton Trans*. **1981**, 1678.
(8) (a) Vance, A. L.; Alcock, N. W.; Busch, D. H.; Heppert, J. A. *Inorg. Chem*. **1997**, *36*, 5132. (b) Rybak-Akimova, E. V.; Nazarenko, A. Y.; Silchenko, S. S. *Inorg. Chem*. **1999**, *38*, 2974.
(9) (a) Drew, M. G. B.; Rodgers, A.; McCann, M.; Nelson, S. M. *J. Chem. Soc., Chem. Commun*. **1978**, 415. (b) Brooker, S.; Croucher, P. D. *J. Chem. Soc., Chem. Commun*. **1993**, 1278.
(10) Esteban, D.; Bañobre, D.; de Blas, A.; Rodríguez-Blas, T.; Bastida, R.; Macías, A.; Rodríguez, A.; Fenton, D. E.; Adams, H.; Mahía, J. *Eur. J. Inorg. Chem.* **2000**, 1445.
(11) Adams, H.; Bailey, N. A.; Carlisle, W. D.; Fenton, D. E.; Rossi, G. *J. Chem. Soc., Dalton Trans*. **1990**, 1271.
(12) Formica, M.; Fusi, V.; Giorgi, L.; Micheloni, M.; Palma, P.; Pontellini, R. *Eur. J. Inorg. Chem*. **2002**, 402.
(13) (a) Alexander, V. *Chem. Rev*. **1995**, *95*, 273. (b) Platas, C.; Avecilla, F.; de Blas, A.; Rodríguez-Blas, T.; Bünzli, J.-C. G. *J. Chem. Soc., Dalton Trans*. **1999**, 1763. (c) Platas, C.; Avecilla, F.; de Blas, A.; Rodríguez-Blas, T.; Geraldes, C. F. G. C.; Tóth, É; Merbach, A. E.; Bünzli, J.-C. G. *J. Chem. Soc., Dalton Trans*. **2000**, 611.
(14) Esteban, D.; Bañobre, D.; Bastida, R.; de Blas, A.; Macías, A.; Rodríguez, A.; Rodríguez-Blas, T.; Fenton, D. E.; Adams, H.; Mahía, J. *Inorg. Chem.* **1999**, *38*, 1937.
(15) Avecilla, F.; Esteban, D.; Platas-Iglesias, C.; De Blas, A.; Rodríguez-Blas, T. *Acta Crystallogr*. **2003**, *C59*, m16.
(16) (a) Cai, S.-H.; Chen, Z.; Wan, H.-L. *J. Phys. Chem. A* **2002**, *106*, 1060. (b) Cerda, B. A.; Hoyau, S.; Ohanessian, G.; Wesdemiotis, C. *J. Am. Chem. Soc*. **1998**, *120*, 2437. (c) Wyttenbach, T.; Witt, M.; Bowers, M. T. *J. Am. Chem. Soc*. **2000**, *122*, 3458. (d) Marino, T.; Russo, N.; Toscano, M. *Inorg. Chem*. **2001**, *40*, 6439.
(17) García, R.; Seco, J. M.; Vázquez, S. A.; Quínoa, E.; Riguera, R. *J. Org. Chem.* **2002**, *67*, 4579.
(18) Esteban, D.; Avecilla, F.; Platas-Iglesias, C.; Mahía, J.; De Blas, A.; Rodríguez-Blas, T. *Inorg. Chem.* **2002**, *41*, 4337.
(19) Wolsey, W. C. *J. Chem. Educ.* **1973**, *50*, A335.

cells. Spectrophotometric titrations were performed in the latter spectrometer connected to an external computer. Typically, a solution of the ligand ($\mathbf{L^1}$ or $\mathbf{L^2}$, $\sim 1.5 \times 10^{-5}$ M) in acetonitrile was prepared (50 mL), and then 50−100 μL aliquots of a solution of $Ba(ClO_4)_2 \cdot 3H_2O$ or $Ba(SCN)_2$ ($\sim 1.5 \times 10^{-3}$ M) in the same solvent were successively added. The stability constant of compound **3** was estimated from a competitive titration with Pb(II): A solution of the $[Pb(\mathbf{L^2})](ClO_4)_2$ complex (50 mL) in acetonitrile was prepared ($\sim 9.2 \times 10^{-6}$ M), and then 60−120 μL aliquots of a solution of $Ba(ClO_4)_2 \cdot 3H_2O$ (1.0×10^{-3} M) in the same solvent were successively added. Plots of molar absorption coefficient as a function of the Ba/ligand ratio gave a first indication of the number and stoichiometry of the complexes formed in solution in every titration; factor analysis[20] was then applied to the data to confirm the number of absorbing species. Eventually, a model for the distribution of species was fitted with a nonlinear least-squares algorithm to give stability constants using the computer program SPECFIT.[21]

X-ray Data Collections and Structure Determinations 3 and 4. Three-dimensional X-ray data were collected at room temperature on a Bruker SMART 1000 CCD diffractometer by the $\phi-\omega$ scan method. Reflections were measured at room temperature from a hemisphere of data collected of frames each covering 0.3° in ω. Of the 10869 and 22541 reflections measured for complexes **3** and **4**, respectively, all of which were corrected for Lorentz and polarization effects and for absorption by semiempirical methods based on symmetry-equivalent and repeated reflections, 5760 and 6338 independent reflections exceeded the significance level $|F|/\sigma(|F|) > 4.0$, respectively. Complex scattering factors were taken from the program package SHELXTL.[22] The structures were solved by direct methods and refined by full-matrix least-squares methods on F^2. The hydrogen atoms were included in calculated positions and refined by using a riding mode, except the hydrogen atoms H(1N), H(2N), H(3N), and H(4N) for **3**, and H(1N), H(2N), H(3N), H(4N), H(1S), and H(2S) for **4**, which were first located in a difference electron density map, then fixed to the distance obtained from the corresponding heteroatom, and finally freely refined. Refinement converged with allowance for thermal anisotropy of all non-hydrogen atoms in all compounds. Minimum and maximum final electron densities are the following: −0.858 and 1.120 for **3** and −0.506 and 0.577 e Å^{-3} for **4**. The structure of **3** presents a disorder on four carbon atoms of the crown moiety and on one oxygen atom of the coordinated perchlorate group, and the structure of **4** presents a slight disorder on a carbon atom of the crown moiety; 213 (**3**) and 38 (**4**) restraints had to be imposed, respectively. These disorders have been resolved, and the atomic sites have been observed and refined with anisotropic atomic displacement parameters in each case. The sites occupancy factors were 0.38921 for C(4A) and C(3A), 0.60181 for C(8A), 0.51160 for C(9A), and 0.83592 for O(8A) (compound **3**) and 0.52803 for C(2A) (compound **4**). Crystal data and details on data collection and refinement are summarized in Table 1.

Computational Methods. The investigation of the $[Ba(\mathbf{L^2})]^{2+}$ system was initiated with molecular mechanics and molecular dynamics studies by using the MM+ force field, as implemented in ChemBats3D.[23] These preliminary studies allowed us to obtain a number of initial geometries for the $[Ba(\mathbf{L^2})]^{2+}$ *syn* and *anti* isomers. Selected MM+ geometries were fully optimized by using B3LYP density functional model,[24,25] with the LanL2MB basis set that includes the STO-3G[26,27] basis set for the ligand atoms and the quasirelativistic Los Alamos[28−30] effective core potential (ECP) for barium.[31] Single point energy calculations were performed on all the B3LYP/LanL2MB optimized structures by using the LanL2DZ basis set that includes the Dunning/Huzinaga full double-ζ (D95)[32] basis set for the ligand atoms and the Los Alamos ECP for barium. Most stable geometries for the *syn* and *anti* diastereoisomers were fully reoptimized at the B3LYP/LanL2DZ level of theory. The relative free energies of the two isomers of $[Ba(\mathbf{L^2})]^{2+}$ were calculated in vacuo at the B3LYP/LanL2DZ level, including nonpotential energy (NPE) contributions (that is, zero point energy and thermal terms) obtained by frequency analysis. Solvent effects were evaluated by using the polarizable continuum model (PCM). In particular, we selected the C-PCM variant[33] that, employing conductor rather than dielectric boundary conditions, allows a more robust implementation. The solute cavity is built as an envelope of spheres centered on atoms or atomic groups with appropriate radii. The cavitation and dispersion nonelectrostatic contributions to the energy and energy gradient were omitted. Final free energies include both electrostatic and nonelectrostatic contributions. The NMR shielding tensors of the two isomers of $[Ba(\mathbf{L^2})]^{2+}$ were calculated at the B3LYP/LanL2DZ and B3LYP/

Table 1. Crystallographic Details for Compounds **3** and **4**

	3	**4**
formula	$C_{26}H_{40}BaCl_2N_4O_{12}$	$C_{28}H_{42}BaN_6O_5S_2$
fw	808.86	744.14
space group	$P\bar{1}$ (No. 2)	$P2_1/n$ (No. 14)
cryst syst	triclinic	monoclinic
a, Å	10.467	9.954(5)
b, Å	10.4755(2)	29.193(5)
c, Å	16.9911(3)	11.313(5)
α, deg	85.075(1)	90
β, deg	80.907(1)	91.371(5)
γ, deg	61.627(1)	90
V, Å^3	1618.47(4)	3286(2)
Z	2	4
T, K	293(2)	293(2)
λ, Å (Mo Kα)	0.71073	0.71073
D_{calcd}, g/cm^3	1.660	1.504
μ, mm^{-1}	1.458	1.380
R_{int}	0.0295	0.0305
reflns measured	7715	8113
reflns obsd	5760	6338
final *R* indices	R1 = 0.0489	R1 = 0.0351
$[I > 2\sigma(I)]^a$	wR2 = 0.0993	wR2 = 0.0665
final *R* indices	R1 = 0.0764	R1 = 0.0543
(for all data)	wR2 = 0.1131	wR2 = 0.0728

^{a} $R1 = \sum||F_o| - |F_c|/\sum|F_o|$. $wR2 = \{\sum[w(|F_o|^2 - |F_c|^2)^2]/\sum[w(F_o^4)]\}^{1/2}$.

(20) Malinowski, E. R.; Howery, D. G. *Factor Analysis in Chemistry*; J. Wiley: New York, 1980.
(21) Gampp, H.; Maeder, M.; Meyer, C. J.; Zuberbühler, A. D. *Talanta* **1986**, *33*, 943.
(22) Sheldrick, G. M. *SHELXTL: An Integrated System for Solving and Refining Crystal Structures from Diffraction Data (Revision 5.1)*; University of Göttingen: Göttingen, Germany, 1997.
(23) *CS Chem 3D Pro, version 5.0; Molecular Modeling and Analysis Program*; CambridgeSoft Corporation: Cambridge, MA, 1999. http://www.camsoft.com.
(24) Becke, A. D. *J. Chem. Phys.* **1993**, *98*, 5648.
(25) Lee, C.; Yang, W.; Parr, R. G. *Phys. Rev. B* **1988**, *37*, 785.
(26) Hehre, W. J.; Stewart, R. F.; Pople, J. A. *J. Chem. Phys.* **1969**, *51*, 2657.
(27) Collins, J. B.; Schleyer, P. v. R.; Binkley, J. S.; Pople, J. A. *J. Chem. Phys.* **1976**, *64*, 5142.
(28) Hay, P. J.; Wadt, W. R. *J. Chem. Phys.* **1985**, *82*, 270.
(29) Wadt, W. R.; Hay, P. J. *J. Chem. Phys.* **1985**, *82*, 284.
(30) Hay, P. J.; Wadt, W. R. *J. Chem. Phys.* **1985**, *82*, 299.
(31) A description of the basis sets and theory level used in this work can be found in: Foresman, J. B.; Frisch, A. E. *Exploring Chemistry with Electronic Structure Methods*, 2nd ed.; Gaussian Inc.: Pittsburgh, PA, 1996.
(32) Dunning, T. H., Jr.; Hay, P. J. In *Modern Theoretical Chemistry*; Schaefer, H. F., Ed.; Plenum: New York, 1976.
(33) Barone, V.; Cossi, M. *J. Phys. Chem. A* **1998**, *102*, 1995.

LanL2DZdp[34,35] levels using the GIAO[36] method. For chemical shift calculation purposes, NMR shielding tensors of tetramethylsilane (TMS) were calculated at the appropriate same level. All DFT calculations were performed by using the Gaussian 98 package (revision A.11.3).[37]

Results

X-ray Crystal Structures. Crystals of **3** and **4** contain the cations $[Ba(\mathbf{L^2})(ClO_4)]^+$ and $[Ba(\mathbf{L^2})(H_2O)(NCS)]^+$, respectively, and one well-separated perchlorate (compound **3**) or thiocyanate group (compound **4**). Figure 1 displays a view of both complex cations, whereas bond lengths and angles of their coordination spheres are compiled in Table 2. In both complexes, the barium ion is 10-coordinate, being bound to the eight available donor atoms of the receptor $\mathbf{L^2}$. In **3**, two oxygen atoms of a bidentate perchlorate group complete the coordination sphere, while in **4** it is completed by the nitrogen atom of a thiocyanate group and the oxygen atom of a water molecule. Distances Ba(1)−O(5) (2.933(4) Å) and Ba(1)−O(6) (3.004(4) Å) found in **3** indicate a very weak coordination of the perchlorate group to the metal ion that it is usually described as "semi-coordination".[38] In both complexes, distances between the barium(II) ion and the oxygen atoms and pivotal nitrogen atoms (N(3) and N(4)) of the crown moiety fall within the ranges observed for the analogous complexes with $\mathbf{L^1}$ (compounds **1** and **2**), while the Ba(1)−N(1) and Ba(1)−N(2) distances are slightly longer in **3** and **4**.[14,15] Unlike compounds **1** and **2**, where the receptor $\mathbf{L^1}$ adopts a *syn* conformation,[14,15] in compounds **3** and **4**, the organic receptor $\mathbf{L^2}$ adopts an *anti* arrangement with both aniline pendant arms disposed on opposite sides of the crown moiety and the barium(II) ion fitted into the crown moiety hole. The distance between both aniline donors [N(1)−N(2)] amounts to 5.691 Å in **3** and to 5.722 Å in **4**, whereas the distance between both pivotal nitrogen atoms [N(3)−N(4)] is 5.825 Å in **3** and 5.908 Å in **4**, which points out that the different nature of the anion present in the complex (thiocyanate or perchlorate) hardly affects the macrocyclic cavity size in these compounds.

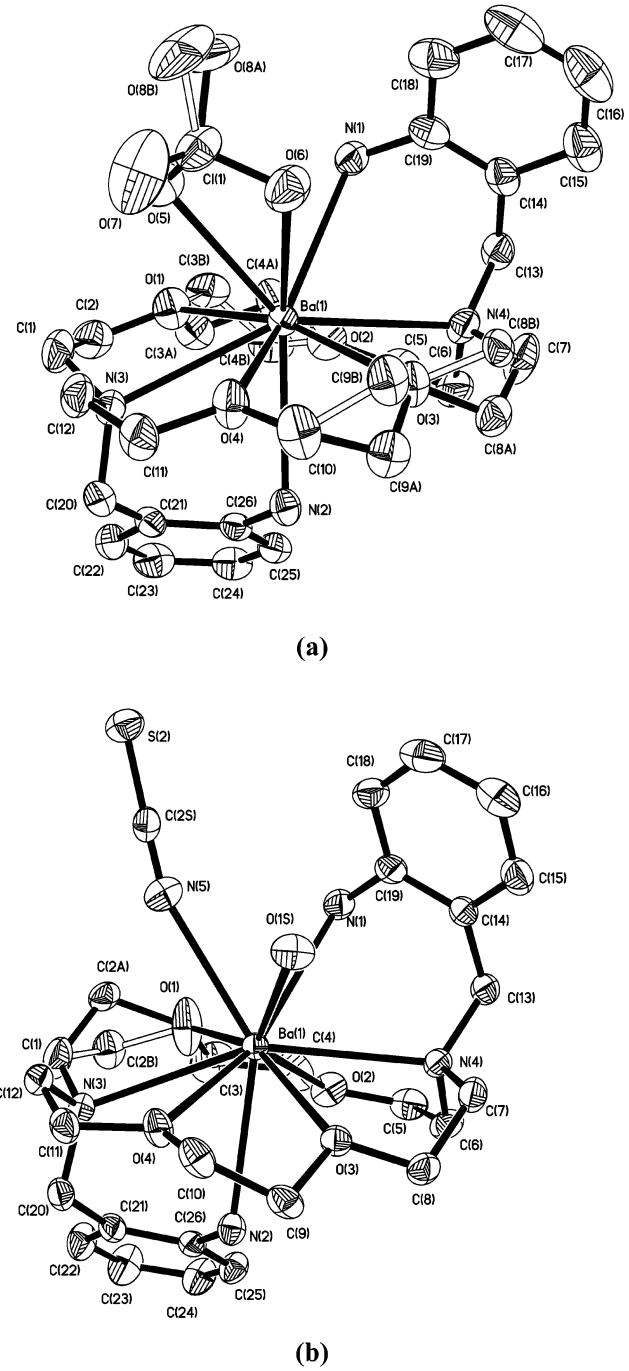

Figure 1. X-ray crystal structures of complexes $[Ba(\mathbf{L^2})(ClO_4)]^+$ (a) and $[Ba(\mathbf{L^2})(H_2O)(NCS)]^+$ (b). Hydrogen atoms are omitted for clarity. The ORTEP plots are at the 30% probability level.

As depicted in Figure 1, the X-ray crystal structures of **3** and **4** present disorders on some of the carbon atoms of the crown moiety, for which two atomic sites have been observed. This situation is probably a consequence of the flexibility of the crown moiety, which can adopt different conformations with similar energy. Likewise, each of the coordinated $N-(CH_2-CH_2)-O$ or $O-(CH_2-CH_2)-O$ units of the macrobicyclic receptor forms five-membered chelate

(34) Check, C. E.; Faust, T. O.; Bailey, J. M.; Wright, B. J.; Gilbert, T. M.; Sunderlin, L. S. *J. Phys. Chem. A* **2001**, *105*, 8111.
(35) This basis set was obtained from the Extensible Computational Chemistry Environment Basis Set Database, Version 2/12/03, as developed and distributed by the Molecular Science Computing Facility, Environmental and Molecular Sciences Laboratory, which is part of the Pacific Northwest Laboratory, P.O. Box 999, Richland, WA 99352, and funded by the U.S. Department of Energy. The Pacific Northwest Laboratory is a multiprogram laboratory operated by Battelle Memorial Institute for the U.S. Department of Energy under Contract DE-AC06-76RLO 1830. http://www.emsl.pnl.gov:2080/forms/basisform.html.
(36) Ditchfield, R. *Mol. Phys*. **1974**, *27*, 789. Wolinki, K.; Hinton, J. F.; Pulay, P. *J. Am. Chem. Soc*. **1990**, *112*, 8251.
(37) Frisch, M. J.; Trucks, G. W.; Schlegel, H. B.; Scuseria, G. E.; Robb, M. A.; Cheeseman, J. R.; Zakrzewski, V. G.; Montgomery, J. A., Jr.; Stratmann, R. E.; Burant, J. C.; Dapprich, S.; Millam, J. M.; Daniels, A. D.; Kudin, K. N.; Strain, M. C.; Farkas, O.; Tomasi, J.; Barone, V.; Cossi, M.; Cammi, R.; Mennucci, B.; Pomelli, C.; Adamo, C.; Clifford, S.; Ochterski, J.; Petersson, G. A.; Ayala, P. Y.; Cui, Q.; Morokuma, K.; Malick, D. K.; Rabuck, A. D.; Raghavachari, K.; Foresman, J. B.; Cioslowski, J.; Ortiz, J. V.; Baboul, A. G.; Stefanov, B. B.; Liu, G.; Liashenko, A.; Piskorz, P.; Komaromi, I.; Gomperts, R.; Martin, R. L.; Fox, D. J.; Keith, T.; Al-Laham, M. A.; Peng, C. Y.; Nanayakkara, A.; Challacombe, M.; Gill, P. M. W.; Johnson, B.; Chen, W.; Wong, M. W.; Andres, J. L.; Gonzalez, C.; Head-Gordon, M.; Replogle, E. S.; Pople, J. A. *Gaussian 98*, revision A.11; Gaussian, Inc.: Pittsburgh, PA, 1998.
(38) Gowda, M. N.; Naikar, S. B.; Reddy, G. K. *Adv. Inorg. Radiochem.* **1984**, *28*, 255.

Table 2. Selected Bond Lengths (Å) and Angles (deg) for Compounds **3** and **4**

		3	
Ba(1)−O(4)	2.765(3)	Ba(1)−N(1)	2.959(4)
Ba(1)−O(3)	2.777(3)	Ba(1)−N(2)	2.959(4)
Ba(1)−O(2)	2.791(3)	Ba(1)−O(6)	3.004(4)
Ba(1)−O(1)	2.792(3)	Ba(1)−N(3)	3.007(4)
Ba(1)−O(5)	2.933(4)	Ba(1)−N(4)	3.027(4)
O(4)−Ba(1)−O(3)	59.40(9)	O(2)−Ba(1)−O(6)	143.86(12)
O(4)−Ba(1)−O(2)	146.87(12)	O(1)−Ba(1)−O(6)	122.89(11)
O(3)−Ba(1)−O(2)	112.73(10)	O(5)−Ba(1)−O(6)	45.70(10)
O(4)−Ba(1)−O(1)	119.29(11)	N(1)−Ba(1)−O(6)	69.58(12)
O(3)−Ba(1)−O(1)	163.36(11)	N(2)−Ba(1)−O(6)	134.28(11)
O(2)−Ba(1)−O(1)	58.17(11)	O(4)−Ba(1)−N(3)	59.04(10)
O(4)−Ba(1)−O(5)	80.98(11)	O(3)−Ba(1)−N(3)	113.85(10)
O(3)−Ba(1)−O(5)	116.63(10)	O(2)−Ba(1)−N(3)	105.40(11)
O(2)−Ba(1)−O(5)	125.53(10)	O(1)−Ba(1)−N(3)	60.55(11)
O(1)−Ba(1)−O(5)	78.05(10)	O(5)−Ba(1)−N(3)	74.35(11)
O(4)−Ba(1)−N(1)	137.40(12)	N(1)−Ba(1)−N(3)	138.96(10)
O(3)−Ba(1)−N(1)	103.04(11)	N(2)−Ba(1)−N(3)	64.57(10)
O(2)−Ba(1)−N(1)	74.45(11)	O(6)−Ba(1)−N(3)	103.88(12)
O(1)−Ba(1)−N(1)	88.28(12)	O(4)−Ba(1)−N(4)	119.34(10)
O(5)−Ba(1)−N(1)	73.45(11)	O(3)−Ba(1)−N(4)	60.63(10)
O(4)−Ba(1)−N(2)	68.61(11)	O(2)−Ba(1)−N(4)	58.03(11)
O(3)−Ba(1)−N(2)	72.82(10)	O(1)−Ba(1)−N(4)	115.25(11)
O(2)−Ba(1)−N(2)	78.31(10)	O(5)−Ba(1)−N(4)	135.80(11)
O(1)−Ba(1)−N(2)	91.11(11)	N(1)−Ba(1)−N(4)	65.53(11)
O(5)−Ba(1)−N(2)	137.30(11)	N(2)−Ba(1)−N(4)	86.26(11)
N(1)−Ba(1)−N(2)	148.21(11)	O(6)−Ba(1)−N(4)	102.41(12)
O(4)−Ba(1)−O(6)	68.15(12)	N(3)−Ba(1)−N(4)	149.71(11)
O(3)−Ba(1)−O(6)	73.07(10)		
		4	
Ba(1)−O(1)	2.740(2)	Ba(1)−N(5)	2.889(3)
Ba(1)−O(4)	2.741(2)	Ba(1)−N(1)	2.961(3)
Ba(1)−O(2)	2.790(2)	Ba(1)−N(4)	2.985(2)
Ba(1)−O(3)	2.7908(19)	Ba(1)−N(2)	3.084(3)
Ba(1)−O(1S)	2.835(3)	Ba(1)−N(3)	3.086(3)
O(1)−Ba(1)−O(4)	116.68(7)	O(4)−Ba(1)−N(4)	120.31(7)
O(1)−Ba(1)−O(2)	58.66(8)	O(2)−Ba(1)−N(4)	60.76(7)
O(4)−Ba(1)−O(2)	136.28(7)	O(3)−Ba(1)−N(4)	61.16(6)
O(1)−Ba(1)−O(3)	155.61(9)	O(1S)−Ba(1)−N(4)	81.60(7)
O(4)−Ba(1)−O(3)	59.22(6)	N(5)−Ba(1)−N(4)	126.22(8)
O(2)−Ba(1)−O(3)	106.06(6)	N(1)−Ba(1)−N(4)	66.33(7)
O(1)−Ba(1)−O(1S)	140.53(9)	O(1)−Ba(1)−N(2)	85.67(9)
O(4)−Ba(1)−O(1S)	75.30(7)	O(4)−Ba(1)−N(2)	66.34(7)
N(2)−Ba(1)−N(3)	62.11(6)	O(2)−Ba(1)−N(2)	69.94(7)
O(2)−Ba(1)−O(1S)	139.08(7)	O(3)−Ba(1)−N(2)	70.59(6)
O(3)−Ba(1)−O(1S)	63.74(6)	O(1S)−Ba(1)−N(2)	130.89(6)
O(1)−Ba(1)−N(5)	75.41(11)	N(5)−Ba(1)−N(2)	141.64(8)
O(4)−Ba(1)−N(5)	92.66(8)	N(1)−Ba(1)−N(2)	142.39(7)
O(2)−Ba(1)−N(5)	122.85(9)	N(4)−Ba(1)−N(2)	92.03(7)
O(3)−Ba(1)−N(5)	127.12(9)	O(1)−Ba(1)−N(3)	59.35(7)
O(1S)−Ba(1)−N(5)	66.25(9)	O(4)−Ba(1)−N(3)	57.33(7)
O(1)−Ba(1)−N(1)	77.89(9)	O(2)−Ba(1)−N(3)	101.43(7)
O(4)−Ba(1)−N(1)	150.98(7)	O(3)−Ba(1)−N(3)	111.14(6)
O(2)−Ba(1)−N(1)	72.61(7)	O(1S)−Ba(1)−N(3)	119.36(7)
O(3)−Ba(1)−N(1)	117.77(6)	N(5)−Ba(1)−N(3)	79.55(8)
O(1S)−Ba(1)−N(1)	78.18(7)	N(1)−Ba(1)−N(3)	130.50(7)
N(5)−Ba(1)−N(1)	65.67(8)	N(4)−Ba(1)−N(3)	153.37(7)
O(1)−Ba(1)−N(4)	116.01(7)		

rings $\overline{\text{Ba−N−C−C−O}}$ or $\overline{\text{Ba−O−C−C−O}}$ that can adopt δ or λ conformations. In the following, we will use the notations δ' and λ' for the two enantiomeric forms of the five-membered chelate rings $\overline{\text{Ba−O−C−C−O}}$. Inspection of the crystal structure data reveals that for the major atomic sites (labeled as A in Figure 1) compounds **3** and **4** present $(\delta\lambda'\delta)(\delta\lambda'\lambda)$ and $(\lambda\lambda'\delta)(\lambda\lambda'\delta)$ conformations, respectively, where each term within parentheses represents the conformations of the three five-membered chelate rings formed by one of the $N-(CH_2)_2-O-(CH_2)_2-O-(CH_2)_2-N$ moiety of the ligand backbone.

Table 3. ^{1}H and ^{13}C NMR Data (δ, ppm) for Compounds **3** and **4** in CD_3CN Solution (200 MHz)

	3[a]	**4**[a]		**3**[b]
H2	7.06 (d, 2H)	7.06 (d, 2H)	C1	145.1
H3	7.29 (t, 2H)	7.25 (t, 2H)	C2	118.5
H4	6.97 (t, 2H)	6.92 (t, 2H)	C3	130.2
H5	7.25 (d, 2H)	7.22 (d, 2H)	C4	121.7
H7	3.64 (s, 4H)	3.65 (s, 4H)	C5	133.3
H8	2.86 (t, 8H)	2.86 (t, 8H)	C6	120.1
H9	3.72 (t, 8H)	3.73 (t, 8H)	C7	56.5
H10	3.57 (s, 8H)	3.57 (s, 8H)	C8	56.0
			C9	69.0
			C10	70.6

[a] Data recorded at 348 K. [b] Data recorded at 298 K.

^{1}H and ^{13}C NMR Spectra of Compounds 3 and 4. The solution behavior of compounds **3** and **4** in acetonitrile was investigated by ^{1}H NMR spectroscopy in the temperature range 228−348 K (see Chart 1 for labeling scheme). At 348 K, the ^{1}H NMR spectra of **3** and **4** display only four resonances of aliphatic protons (Table 3): H7 and H10 appear as the expected singlets, while H8 and H9 do as triplets. By comparison with the spectrum of the free receptor $\mathbf{L^2}$,[14] these signals are shifted downfield by 0.08−0.25 ppm, whereas the singlet signal of amine protons is shifted upfield by 0.70 (**3**) and 0.60 ppm (**4**) as a consequence of the coordination of the amine groups to the Ba(II) ion. Upon decreasing the temperature, the signals corresponding to the H7−H10 protons gradually broaden, reflecting intramolecular conformational exchange processes. Despite the increasing complexity of the spectra on decreasing the temperature, some temperature dependent spectral changes can be analyzed and interpreted. At 288 K, the signals of the H8 protons ($H8_{axial}$ and $H8_{equatorial}$) of compounds **3** and **4** appear as two different peaks with equal intensity. These resonances gradually broaden above this temperature, and finally, they coalesce at ca. 304 K, reflecting an intramolecular $\delta \leftrightarrow \lambda$ conformational interconversion in the $\overline{\text{N−CH}_2\text{−CH}_2\text{−O−Ba}}$ metal-bound moiety.[39] From the coalescence temperature of the diasterotopic signals $H8_{axial}$ and $H8_{equatorial}$, which at elevated temperature are equivalent, we estimate identical activation barriers of $\Delta G^{\ddagger} = 62 \pm 5$ kJ mol^{-1} for this intramolecular dynamic process in **3** and **4**.[40] Similar intramolecular dynamic processes are probably responsible for the broadening of the signals corresponding to the H7, H9, and H10 protons below 348 K, but a detailed line shape analysis and a determination of $\Delta G^{\ddagger}$ have not been possible due to overlaps with other proton signals.

Upon decreasing the temperature below 288 K, the signal due to the amine protons also broadens for both compounds **3** and **4**, and finally splits into two different resonances, which indicates the presence of two different isomers of **3**

(39) Schlager, O.; Wieghardt, K.; Grondey, H.; Rufinska, A.; Nuber, B. *Inorg. Chem.* **1995**, *34*, 6440.
(40) Günther, H. In *NMR Spectroscopy*, 2nd ed.; J. Wiley & Sons: Chichester, U.K., 1995; Chapter 9.

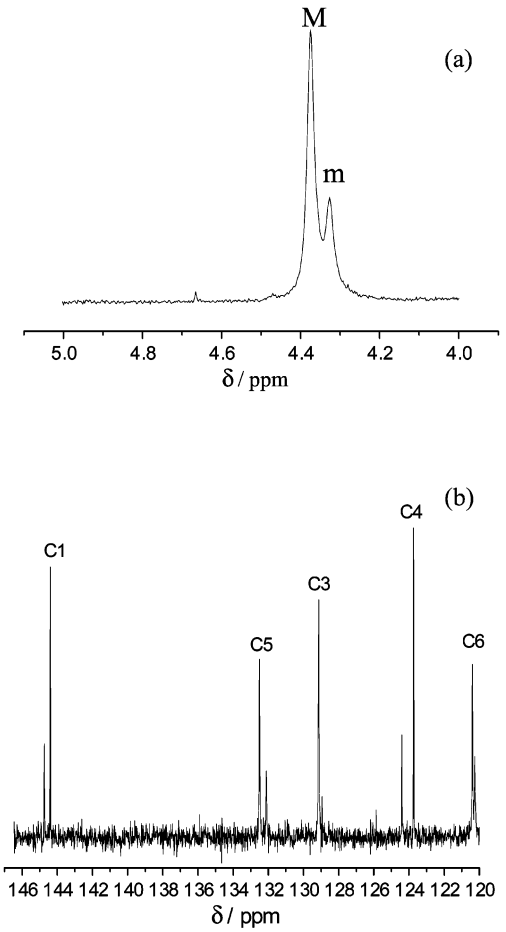

Figure 2. (a) Part of the ^{1}H NMR spectrum (CD_3CN, 228 K) of compound **3** showing the resonance of the amine protons corresponding to the *syn* and *anti* isomers. (b) Part of the ^{13}C NMR spectra (CD_3CN, 228 K) of compound **3**.

and **4** in acetonitrile solution labeled as major (M) and minor (m) isomers (see Figure 2). This behavior is not observed for the barium complexes with $\mathbf{L^1}$ (compounds **1** and **2**), for which at 228 K only one resonance due to the amine protons is observed at 4.42 (**1**) or 4.61 (**2**) ppm, suggesting the presence of a single isomer in acetonitrile solution.[14] The ^{13}C NMR spectra of compound **3** recorded in acetonitrile solution at 295 K present four resonances of aliphatic carbons and six resonances of aromatic ones (Table 3). However, when the spectrum is recorded at 228 K most of carbon signals of aromatic nuclei split into two peaks with different intensities, which again provides evidence of the presence of two species in acetonitrile solution that are in fast exchange at room temperature (Figure 2). The low solubility of **4** in acetonitrile solution has prevented us from performing a similar ^{13}C NMR study for this compound.

Density Functional Theory Calculations. The conformational behavior of the Ba(II) complexes with $\mathbf{L^2}$ was investigated both in vacuo and in acetonitrile solution by means of DFT calculations by using the B3LYP model. Since compound **3** has been shown to behave as a 2:1 electrolyte in acetonitrile solution,[14] we performed our calculations on the $[Ba(\mathbf{L^2})]^{2+}$ system. As there is not any all-electron basis set for barium, the effective core potential of Wadt and Hay

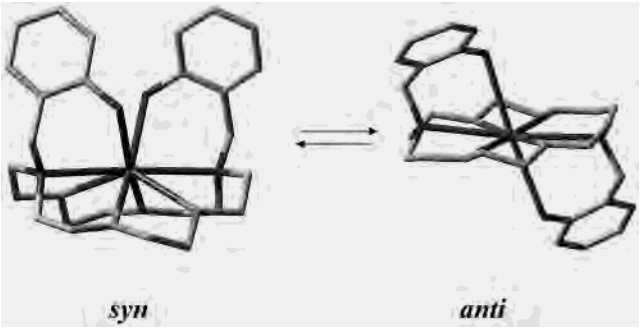

Figure 3. Structures of the two isomers of $[Ba(\mathbf{L^2})]^{2+}$ obtained from DFT calculations at the B3LYP/LanL2DZ level in acetonitrile solution.

(Los Alamos ECP) included in the LanL2DZ basis set was applied in these calculations. Compared to the all-electron basis set, ECPs account for relativistic effects to some extent. It is believed that relativistic effects will become important for the elements from the fourth row of the periodic table. However, while ECPs have been widely used for transition metal compounds, less experience has been gained about alkali-earth metal compounds. Lowest energy geometries located at the B3LYP/LanL2DZ level of theory for the *syn* and *anti* isomers of the $[Ba(\mathbf{L^2})]^{2+}$ system are shown in Figure 3. Although no symmetry constraints were included during the calculations, the resulting structures present C_2 (*syn*) and C_i (*anti*) symmetries. Comparisons of the *anti* conformation obtained from DFT calculations with the X-ray structure of **3** show that the experimental bond distances are well reproduced at the B3LYP/LanL2DZ level (Table 4). The in vacuo optimized structure of the *syn* isomer presents bond distances slightly longer than the experimental values obtained from the X-ray structures of compounds **3** and **4** (Table 4), while the in vacuo optimized structure of the *anti* isomer presents bond distances in very good agreement with the experimental ones. In solution, bond distances slightly decrease, providing a general better agreement with the experimental ones.

From the conformational energies of both isomers (including NPE contributions), we have calculated an in vacuo relative free energy, $\Delta G^\circ_{298K} = G^\circ_{syn} - G^\circ_{anti}$, of -2.60 kcal mol^{-1}. Likewise, from the results obtained in acetonitrile solution we have obtained a relative free energy, $\Delta G^{sol} = G^{sol}_{syn} - G^{sol}_{anti}$, of -3.59 kcal mol^{-1}. These results suggest that the solvation has a significant effect on the isomeric composition, favoring the *syn* isomer. This effect may be due to the different polarity of the two isomers. The *syn* isomer is more polar than the *anti* one and, consequently, is more stabilized by a relatively polar solvent such as acetonitrile.

The conformation of the crown moiety for both isomers obtained from DFT calculations is very different, and it also differs from the one observed in the solid state for **3** and **4**. So, whereas compounds **3** and **4** present, respectively, $(\delta\lambda'\delta)(\delta\lambda'\lambda)$ and $(\lambda\lambda'\delta)(\lambda\lambda'\delta)$ conformations in the solid state (vide supra), the structures of the *syn* and *anti* isomers obtained from DFT calculations present $(\delta\lambda'\delta)(\delta\lambda'\delta)$ (*syn*) and $(\lambda\delta'\delta)(\lambda\lambda'\delta)$ (*anti*) conformations, that are consistent

Table 4. Values of the Mean Bond Distances (Å) of Experimental and Calculated (in Vacuo and in Acetonitrile Solution) Structures of the Two Isomers of **3** and **4**[a]

	syn (B3LYP/LanL2DZ)		*anti* (B3LYP/ LanL2DZ)			
	in vacuo	in solution	in vacuo	in solution	complex **3**[d]	complex **4**[d]
Ba−O	2.850 (0.006)	2.821 (0.002)	2.829 (0.010)	2.815 (0.010)	2.781 (0.016)	2.765 (0.025)
Ba−N[b]	3.016 (0.001)	2.995 (0.001)	2.978 (0.000)	2.963 (0.002)	2.959 (0.000)	2.973 (0.012)
Ba−N[c]	3.067 (0.001)	3.049 (0.000)	3.061 (0.001)	3.050 (0.007)	3.017 (0.010)	3.085 (0.001)

[a] The average values are reported with standard deviations in parentheses. [b] Primary amine. [c] Tertiary amine. [d] From X-ray structures.

Table 5. Experimental and Calculated (GIAO Method) ^{13}C NMR Chemical Shift Values (δ, ppm) for $[Ba(\mathbf{L^2})]^{2+}$

	major (M)[a]	minor (m)[a]	*syn*[b]	*syn*[c]	*anti*[b]	*anti*[c]
C8	54.4	*d*	58.0	55.4	68.2	64.4
C7	54.6	*d*	62.4	58.4	65.2	60.1
C9	67.4	67.6	76.8	74.9	79.1	77.1
C10	68.8	69.8	79.4	75.6	78.4	76.8
C2	119.0	118.7	124.3	120.4	122.5	120.5
C6	120.4	120.2	124.3	120.3	127.5	122.7
C4	123.7	124.4	132.7	129.7	131.9	130.4
C3	129.1	*d*	137.6	135.7	138.1	136.3
C5	132.5	132.1	139.9	136.9	139.8	136.0
C1	144.4	144.7	141.6	140.5	142.7	141.7
AF_i			0.067	0.044	0.083	0.059

[a] Experimental ^{13}C NMR chemical shift values (δ, ppm) as determined at 228 K for compound **3**. [b] Chemical shifts with respect to TMS calculated on in vacuo B3LYP/LanL2DZ optimized geometries at the same computational level. [c] Chemical shifts with respect to TMS calculated on in vacuo B3LYP/LanL2DZ optimized geometries at the B3LYP/LanL2DZdp computational level. [d] Not observed.

with C_2 (*syn*) and C_i (*anti*) symmetries. Conformations found for **3** and **4** in the solid state correspond to C_1 symmetries. The ^{13}C NMR spectra of **3** recorded at 228 K shows 10 signals for the 26 carbon atoms of the ligand backbone corresponding to the major isomer (M), which clearly indicates a higher symmetry than C_1 in solution (Table 5). These results suggest that our barium intermediates **3** and **4** possess a somewhat different structure in the solid state and in solution, probably as a consequence of crystal packing forces in the solid state. Different conformations of five-membered chelate rings in the solid state and in acetonitrile solution have been reported recently for lanthanide cryptates.[41]

Spectrophotometric Titrations. UV−vis spectroscopy is a general method used for the assessment of the coordination environment and for the measurements of stability constants of metal complexes, but it has been less exploited, compared with potentiometric methods, for the study of macrocyclic metal complexes.[42] Incorporating benzo-groups to the ligand backbone increases the absorption coefficients rendering the absorbance useful for spectrophotometric studies. The UV−vis spectra of the free ligands $\mathbf{L^1}$ and $\mathbf{L^2}$, recorded in acetonitrile solution, feature two absorption bands with maxima at 244 and 292 nm ($\mathbf{L^1}$) and 236 and 288 nm ($\mathbf{L^2}$) corresponding to E_2 and B $\pi-\pi^*$ transitions of the substituted aromatic rings, respectively.[43] Upon complexation to Ba(II), both absorption bands experience a blue shift due to the coordination of the amine groups, thus enabling the formation of the complexes in solution to be monitored.

The spectrophotometric titrations of $\mathbf{L^1}$ and $\mathbf{L^2}$ (ca. 1.5×10^{-5} M) with $Ba(ClO_4)_2 \cdot 3H_2O$ or $Ba(SCN)_2$ were performed in acetonitrile over Ba(II)/L molar ratios ranging from 0 to ca. 2.7. The data displayed a single inflection point when the Ba/ligand molar ratio is close to 1 for all titrations, indicating the existence of only one complex species in solution; factor analysis was then applied to the data to confirm the number of absorbing species. The spectrophotometric titrations with $\mathbf{L^1}$ were satisfactory fitted with equilibria 1 or 2, allowing the estimation of the stability constants in acetonitrile solution: $\log \beta_{Ba\mathbf{L1}} = 7.9(6)$ and $\log \beta_{Ba\mathbf{L1}(NCS)} = 8.5(9)$.

$$Ba^{2+} + \mathbf{L^1} \leftrightarrow [Ba(\mathbf{L^1})]^{2+} \quad (1)$$

$$Ba^{2+} + \mathbf{L^1} + SCN^- \leftrightarrow [Ba(\mathbf{L^1})(NCS)]^{+} \quad (2)$$

In the case of Ba(II) complexes with $\mathbf{L^2}$, the $\log \beta$ values are beyond the upper limit of what can be reasonably extracted by a direct spectrophotometric method at ca. 10^{-5} M. In order to estimate the stability constant for the perchlorate compound (**3**), we carried out a competitive titration of $[Pb(\mathbf{L^2})](ClO_4)_2$ with $Ba(ClO_4)_2 \cdot 3H_2O$ in acetonitrile solution. Upon addition of barium perchlorate, the band centered at 236 nm arising from the E_2 $\pi-\pi^*$ transition of the substituted aromatic rings in the lead(II) complex experiments a blue shift, while the one at 288 nm shifts to lower energies. This allowed us to estimate the stability constant defined by equilibrium 3: $\log \beta_{Ba\mathbf{L2}} = 13.6(6)$. The low solubility of the lead(II) thiocyanate has prevented the determination of the stability constant for **4**.

$$Ba^{2+} + \mathbf{L^2} \leftrightarrow [Ba(\mathbf{L^2})]^{2+} \quad (3)$$

These results demonstrate that the bibrachial lariat ethers $\mathbf{L^1}$ and $\mathbf{L^2}$ form stable complexes with Ba(II) in acetonitrile solution. Moreover, the Ba(II) complex with $\mathbf{L^2}$ displays a much larger stability in acetonitrile solution than those with $\mathbf{L^1}$. This is probably due to (i) the increase in available donor atoms of the ligand $\mathbf{L^2}$ for the coordination to Ba(II) compared with $\mathbf{L^1}$, and (ii) a better fit of the Ba(II) ion in the macrocyclic cavity of $\mathbf{L^2}$ compared to $\mathbf{L^1}$, as observed in the solid state structures. The stability constants obtained for the complexes with $\mathbf{L^1}$ point out that the nature of the counterion (thyocyanate or perchlorate) does not significantly affect the stability of the complexes.

Discussion

In a previous work, we reported the synthesis of the lateral macrobicycles $\mathbf{L^3}-\mathbf{L^6}$ (see Chart 1). We have found that

(41) Rodríguez-Cortiñas, R.; Avecilla, F.; Platas-Iglesias, C.; Imbert, D.; Bünzli, J.-C. G.; de Blas, A.; Rodríguez-Blas, T. *Inorg. Chem.* **2002**, *41*, 5336.
(42) Izatt, R. M.; Pawlak, K.; Bradshaw, J. S. *Chem. Rev.* **1995**, *95*, 2529.
(43) Silverstein, R. M.; Bassler, C. *Spectrometric Identification of Organic Compounds*; Wiley: New York, 1967.

these macrobicyclic receptors cannot be prepared by a direct reaction between the organic precursors, the diamine [*N*,*N*′-bis(2-aminobenzyl)-1,10-diaza-15-crown-5 (**L**^{1}) or *N*,*N*′-bis(2-aminobenzyl)-4,13-diaza-18-crown-6 (**L**^{2})], and the corresponding dialdehyde (2,6-diformylpyridine or 2,6-diformyl-4-methylphenol). However, barium can act as an effective template in these reactions, thereby facilitating the formation of the desired macrobicycles in high yields.[14] The reason for this emerges from the conformation that the diamine precursor possesses: an *anti* arrangement leads to acyclic products as the majority ones, whereas the *syn* conformation favors the cyclization. In absence of any metal cation, both diamines (**L**^{1} and **L**^{2}) dispose their aniline groups in an *anti* arrangement.[10,18] To force them to the *syn* conformation requires the presence of ionic species that place both amine groups pointing in the same direction either by their ability to coordinate the corresponding diamine or by the formation of hydrogen bonds. When the barium cation is present in the reaction medium, the expected *syn* conformation was found for the intermediates of macrobicycles **L**^{3} and **L**^{4}, derived from diamine **L**^{1}, both in the solid state and in solution.[14,15] The structural analysis of the corresponding intermediates ([Ba(**L**^{1})]$(ClO_4)_2$ (compound **1**) and [Ba(**L**^{1})$(NCS)_2$] (compound **2**)), based on the study of the X-ray crystal structures and variable temperature ^{1}H NMR spectroscopy experiments, indicate that the expected *syn* conformation is the only one found in solution during the synthesis of the desired macrobicycles.[14,15] The large ionic radius of this metal ion, that is too big to lie into the hole of the crown moiety of **L**^{1}, together with its preference for high coordination numbers are the key features responsible for the *syn* conformation of **L**^{1} in the presence of this cation. Since both barium(II) perchlorate and barium(II) thiocyanate have been also revealed as effective template agents in the synthesis of macrobicycles **L**^{5} and **L**^{6},[14,18] derived from the larger diamine precursor **L**^{2}, one would expect a similar behavior for the analogous intermediates ([Ba(**L**^{2})(ClO_4)](ClO_4) (compound **3**) and [Ba(**L**^{2})$(H_2O)(NCS)$](SCN) (compound **4**)). However, the data presented here in the Results section indicate that in the solid state the diamine precursor **L**^{2} presents an "unexpected" *anti* conformation in these intermediates **3** and **4**. Now, the larger size of the crown moiety hole in **L**^{2} allows the barium(II) ion to be placed into this hole, favoring the *anti* conformation. If **3** and **4** would also adopt an *anti* conformation in solution, the reaction to give the macrobicycles **L**^{5} and **L**^{6} should not proceed. Therefore, the effectiveness of the barium(II) ion as a template to obtain macrobicycles **L**^{5} and **L**^{6} provides a first indication of the presence (at least to some extent) of a *syn* isomer in solution. This hypothesis is confirmed by the variable temperature ^{1}H and ^{13}C NMR spectra of **3** and **4**, which demonstrate the presence of two different isomers in acetonitrile solution. Furthermore, DFT calculations performed at the B3LYP/LanL2DZ level predict two minimum energy conformations for the [Ba(**L**^{2})]$^{2+}$ system corresponding to *syn* and *anti* isomers. These data can be explained because the Ba(II) ion fits quite well inside the crown moiety hole of **L**^{2}, which makes the existence of an equilibrium between *syn* and *anti* isomers in acetonitrile solution possible:

$$[\mathrm{Ba}(\mathbf{L}^{2})]^{2+}_{syn} \leftrightarrow [\mathrm{Ba}(\mathbf{L}^{2})]^{2+}_{anti} \tag{4}$$

The equilibrium constant corresponding to eq 4 may be written as

$$K_{\mathrm{eq}} = \frac{\left[[\mathrm{Ba}(\mathbf{L}^{2})]_{anti}{}^{2+}\right]}{\left[[\mathrm{Ba}(\mathbf{L}^{2})]_{syn}{}^{2+}\right]} = \frac{x_{anti}}{x_{syn}} \tag{5}$$

where x_{anti} and x_{syn} are the mole fractions of the *syn* and *anti* species, respectively. The reaction enthalpy, $\Delta H°$, and reaction entropy, $\Delta S°$, for the equilibrium can be obtained from the temperature dependence of K_{eq} via

$$\ln K_{\mathrm{eq}} = \frac{\Delta S°}{R} - \frac{\Delta H°}{RT} \tag{6}$$

In order to obtain the thermodynamic parameters for the equilibrium, therefore, it is necessary to relate the measured NMR spectra to the equilibrium constant. On the basis of the DFT calculations already described, which predict the *syn* isomer as the minimum energy conformation, we tentatively assign the major species existing in acetonitrile solution (M) to the *syn* species, while the minor species (m) is assigned to the *anti* one. Further support for this assignment comes from the position of the ^{1}H NMR signals corresponding to the NH_2 groups in compounds **1**−**4**: At 228 K, compounds **3** and **4** show two resonances for these protons at 4.37 (M) and 4.33 (m) ppm (compound **3**) and at 4.62 (M) and 4.37 (m) ppm (compound **4**), while **1** and **2** display a single resonance due to these protons at 4.42 and 4.61 ppm, respectively. In principle, no distinct region on the δ scale can be assigned to the resonances of exchangeable protons since the position of these resonance signals is strongly dependent upon the medium and temperature. However, the position of the NH_2 resonances in **1** and **2**, where only *syn* isomers occur, is nearly identical to that observed for the M isomer in **3** and **4**, respectively, thereby supporting our assignment.

Aiming to further validate this attribution, the ^{13}C NMR shielding constants of both isomers of [Ba(**L**^{2})]$^{2+}$ were calculated at the B3LYP/LanL2DZ level by using the GIAO method and compared with the ^{13}C NMR shifts of the major species in solution (Table 5), for which the expected 10 signals are observed in the ^{13}C NMR spectrum of **3**. An analogous comparison between the calculated ^{13}C NMR shifts and the experimental ones observed for the m isomer was not performed since only 7 of the 10 expected resonances for this isomer are observable in the ^{13}C NMR spectrum of **3**. The calculated ^{13}C shifts of the *syn* isomer provide a general better agreement with the experimental data of the M isomer (Table 5), as evidenced by the lower AF_i agreement factors obtained (Table 5, $AF_i = [\sum(\delta_{\mathrm{exp}} - \delta_{\mathrm{calc}})^2/\sum(\delta_{\mathrm{exp}})^2]^{1/2}$ where δ_{exp} and δ_{calc} denote the experimental and calculated ^{13}C NMR shifts, respectively).[44] The ^{13}C NMR shielding constants of both isomers of [Ba(**L**^{2})]$^{2+}$ were also

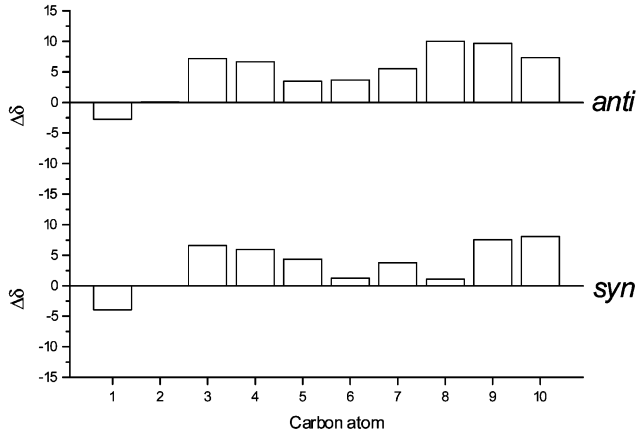

Figure 4. Differences between the calculated and experimental (GIAO method) ^{13}C NMR chemical shifts for the *syn* and *anti* isomers as obtained at the B3LYP/ LanL2DZdp computational level.

calculated at the B3LYP/LanL2DZdp level (Table 5) to investigate whether the introduction of polarization functions affects the agreement between the experimental and calculated ^{13}C NMR shifts. The results show a dramatic improvement of the AF_i agreement factors for both isomers with again a general better agreement between the experimental shifts of the M species and those calculated for the *syn* isomer (Table 5). Figure 4 shows a plot of differences between calculated and experimental ^{13}C NMR shift values for the two isomers of $[Ba(\mathbf{L^2})]^{2+}$ ($\Delta\delta$) obtained at the B3LYP/ LanL2DZdp level, where it is possible to appreciate considerable larger deviations from the experimental values for the C6, C7, and C8 carbon atoms of the *anti* isomer than for the same nuclei in the *syn* one. Although a more rigorous calculation of the ^{13}C NMR shielding constants should involve Boltzmann-averaged GIAO ^{13}C NMR chemical shift calculations[45] for the different conformational states with *syn* and *anti* geometries in dynamic equilibrium, these results support the assignment of the M isomer to the *syn* isomer in acetonitrile solution. The equilibrium constant, K_{eq}, was then obtained at several temperatures between 228 and 268 K for each of the two complexes studied from the integrations of the ^{1}H NMR signals due to the primary amine protons (Figure 3). The ratio between the intensity of the peaks corresponding to the *syn* and *anti* species was found to be constant within the experimental error in the range of temperatures studied. This indicates that $\Delta S^\circ \approx 0$ for the interconversion process described by eq 4, in agreement with an intramolecular interconversion. From our ^{1}H NMR data in acetonitrile solution, we obtain $K_{eq} = 0.34(1)$ and 0.18(2) for **3** and **4**, respectively (equilibrium 5). These results point out that for both barium intermediates (**3** and **4**) the *syn* isomer predominates in acetonitrile solution at any temperature.

Conclusions

Compounds $[Ba(\mathbf{L^2})(ClO_4)](ClO_4)$ (**3**) and $[Ba(\mathbf{L^2})(H_2O)(NCS)](SCN)$ (**4**), which are intermediates in the synthesis of the lateral macrobicycles $\mathbf{L^5}$ and $\mathbf{L^6}$, present an *anti* conformation in the solid state, but they exist in solution as a mixture of *syn* and *anti* isomers. The *syn* isomer predominates in solution for both perchlorate and thiocyanate complexes, but the presence of a different counterion affects the dynamic equilibrium between the *syn* and *anti* isomers. The solution behavior of these complexes allows us to rationalize the role of the barium(II) ion as an effective template agent in the formation of $\mathbf{L^5}$ and $\mathbf{L^6}$, since the formation of cyclic products is favored by the *syn* orientation of the pendant arms forced by the Ba(II) ion.

Frequently, X-ray crystal structures of intermediates are used to rationalize processes that take place in solution. This study also wants to take a firm stand that care should be taken when solution processes are rationalized on the basis of X-ray structures, since the structures in the solid state and in solution may be dramatically different.

Acknowledgment. The authors thank Xunta de Galicia (PGIDT00MAM10302PR) for generous financial support. The authors are indebted to Centro de Supercomputación of Galicia (CESGA) for providing computer facilities.

Supporting Information Available: X-ray crystallographic files in CIF format for **3** and **4**. Optimized Cartesian coordinates (Å) of the two isomers of $[Ba(\mathbf{L^2})]^{2+}$ complexes in vacuo and in acetonitrile solution. This material is available free of charge via the Internet at http://pubs.acs.org.

IC034266T

(44) Willcott, M. R.; Lenkinski, R. E.; Davis, R. E. *J. Am. Chem. Soc*. **1972**, *94*, 1742. Davis, R. E.; Willcott, M. R. *J. Am. Chem. Soc*. **1972**, *94*, 1744.

(45) Barone, G.; Duca, D.; Silvestri, A.; Gomez-Paloma, L.; Riccio, R.; Bifulco, G. *Chem. Eur. J*. **2002**, *8*, 3240. Barone, G.; Gomez-Paloma, L.; Duca, D.; Silvestri, A.; Riccio, R.; Bifulco, G. *Chem. Eur. J*. **2002**, *8*, 3233.